Refining Near-Surface Seismic Structure in the San Francisco Community Velocity Model (SFCVM)

Poster #073

Anupam Patel[1,2] & Kim B. Olsen[1]

[1]San Diego State University (apatel7716@sdsu.edu), [2]University of California San Diego

Background

What?
We optimize the shallow velocity structure in the San Francisco Community Velocity Model (SFCVM version 26).

Why?
Because shallow (≲ 3–4 km) shear-wave velocity (Vs) is poorly constrained in tomographic and geologic models, yet strongly controls seismic response; improving the shallow structure reduces simulation–observation misfit, yielding more accurate ground-motion predictions.

How?
For each event, we apply Vs30-constrained velocity tapers (VTs) at depths ranging from 0 to 4000 m. A low-velocity taper (LVT) reduces velocity, while a high-velocity extension (HVE) increases it to depths of up to 1500 m. Using physics-based ground motion simulations, we compute Fourier amplitude spectra (FAS) and velocity- and acceleration-envelope measures at each recording site for a range of taper depths. We then combine these measures into a site-specific composite error metric to identify the taper depth that minimizes the overall bias.

Model Region

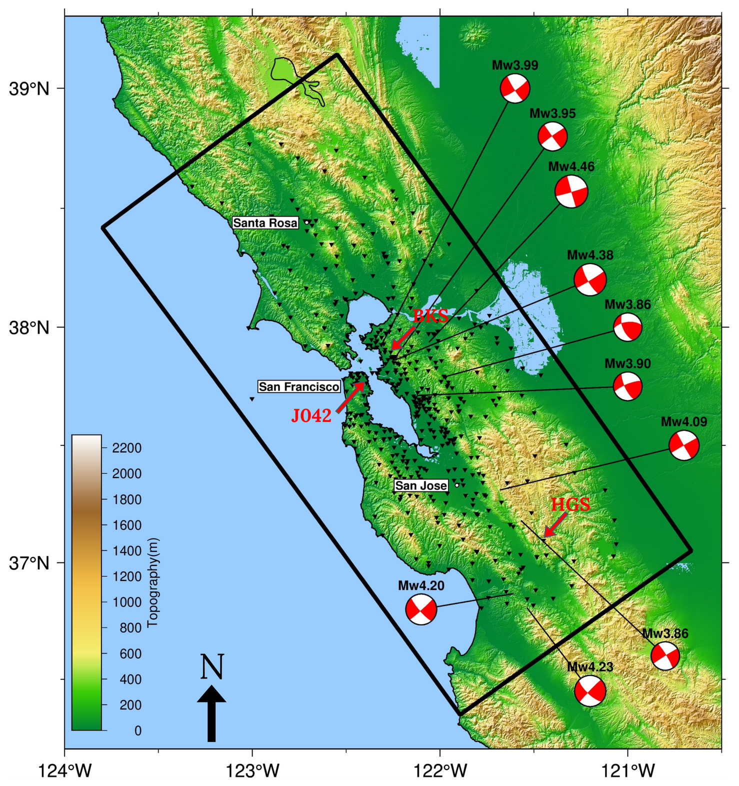

Figure 1: Model domain (rectangle). Shading depicts surface topography. Beach balls show the focal mechanisms and epicenters of the 10 validation events. Black triangles show strong motion stations.

We simulate 10 M3.8-4.5 validation events using AWP-ODC (Cui et al., 2013) with a discontinuous mesh (Nie et al., 2017) and topography using a curvilinear mesh (O'Reilly et al., 2022).

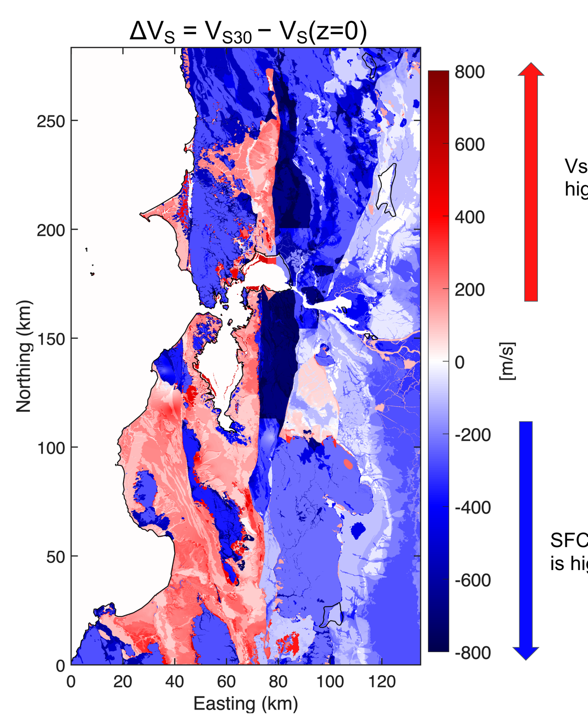

Note that the surface Vs in the SFCVM (v26) is generally high compared to Vs30 except near the San Francisco Bay or in the southwest region. This spatial variability suggests opportunities for model improvement and motivates site-specific, rather than uniform, modifications to shallow velocities.

Figure 2: Difference between Vs30 (Thompson et al., 2018) and surface Vs of SFCVM (v26).

LVT Restores Underpredicted Amplitudes

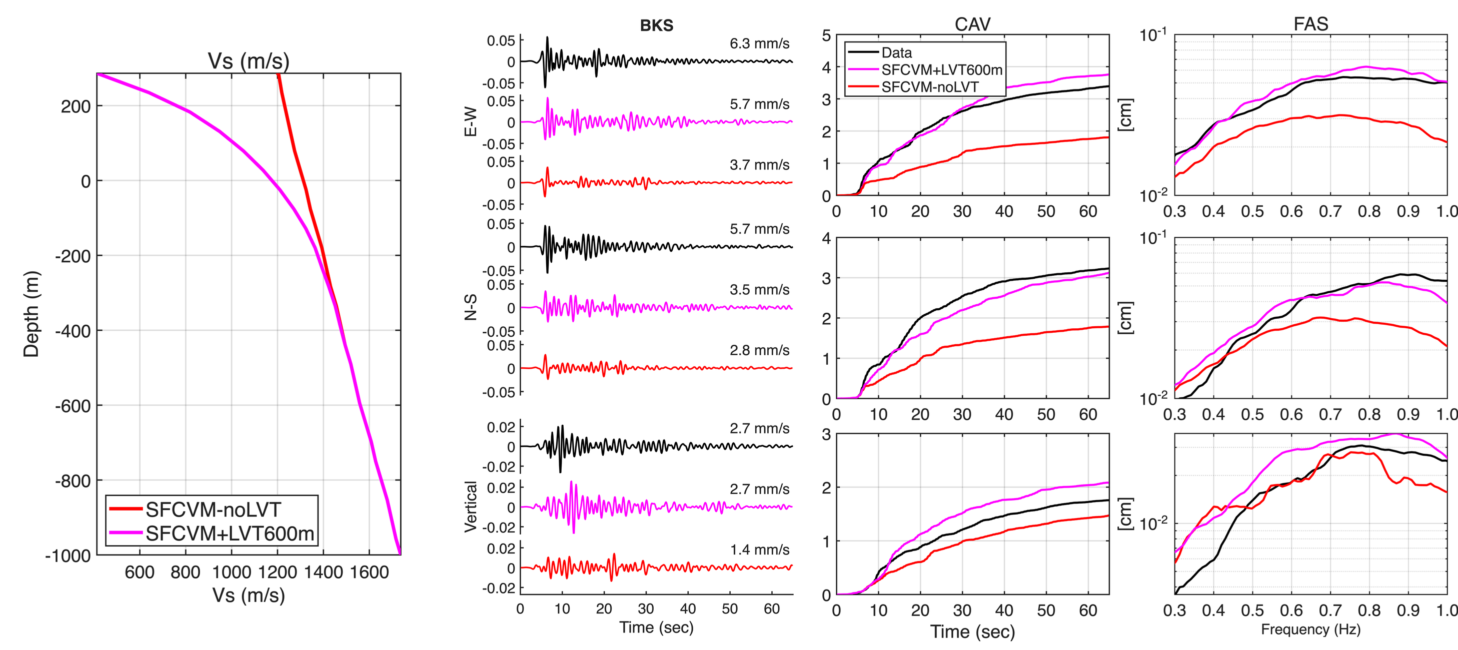

Figure 3: LVT (left) and the effects on ground motions at station BKS (see Fig. 1 for location) (right) for a fixed tapering depth of 600 m using the 2018/01/04 Mw4.38 event.

HVE Reduces Localized Overprediction

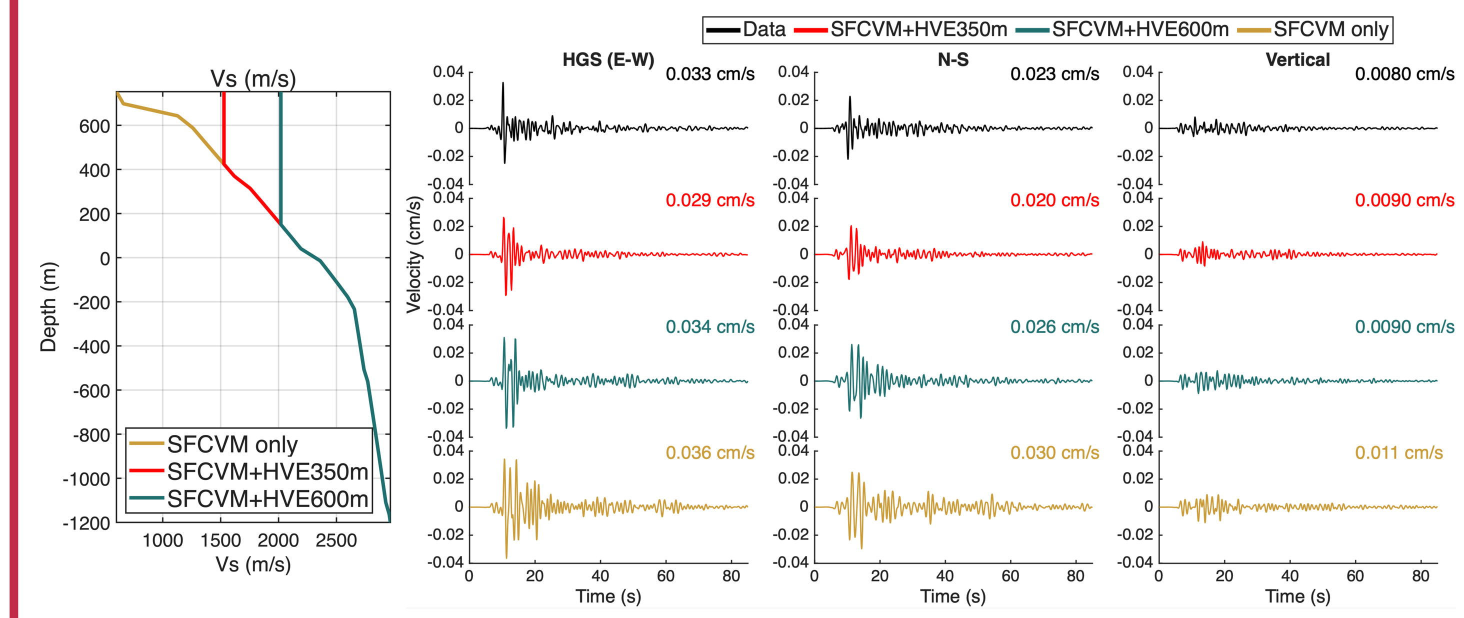

Figure 4: Comparison of velocity profiles and simulated waveforms for the reference SFCVM and the 350 m and 600 m HVE models for the 2021/01/17 Mw4.2 event.

Error Metric: Estimation of Optimal Taper Depth

Error type	Metric name	Weight
Fourier Amplitude Spectrum	FAS_E	1
	FAS_N	1
	FAS_Z	1
Velocity Envelope RMS	VER_E	½
	VER_N	½
	VER_Z	½
Acceleration Envelope RMS	AER_E	½
	AER_N	½
	AER_Z	½

Composite Error:

$$\xi = \frac{\sum_{i=1}^{9} \varepsilon_i w_i}{\sum_{i=1}^{9} w_i}$$

Lower ξ is better; ξ = 0 is a perfect match

FAS Error:

$$\varepsilon_{\mathrm{FAS},j} = \frac{1}{N_f} \sum_{f=1}^{N_f} \left| \log_{10}\left(\frac{\mathrm{FAS}_{\mathrm{syn},j}[f]}{\mathrm{FAS}_{\mathrm{obs},j}[f]} \right) \right|$$

Envelope Error:

$$\varepsilon_{\mathrm{ER},j} = \frac{\sum_{i=1}^{N_t} w[i] b_j[i]}{\sum_{i=1}^{N_t} w[i]}$$

$$w[i] = \sqrt{\mathrm{RMS}_{\mathrm{syn},j}[i]^2 + \mathrm{RMS}_{\mathrm{obs},j}[i]^2} \qquad b_j[i] = \left| \log_{10}\left(\frac{\mathrm{RMS}_{\mathrm{syn},j}[i] + \delta}{\mathrm{RMS}_{\mathrm{obs},j}[i] + \delta} \right) \right|_{\delta = 10^{-12}}$$

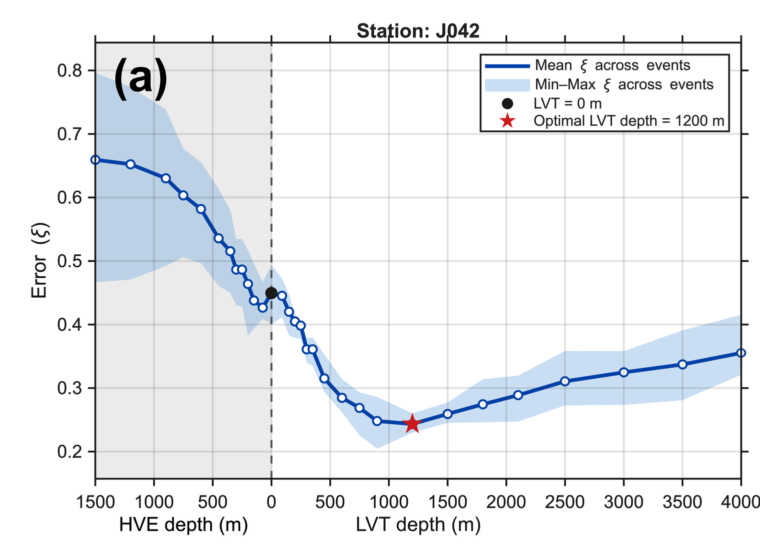

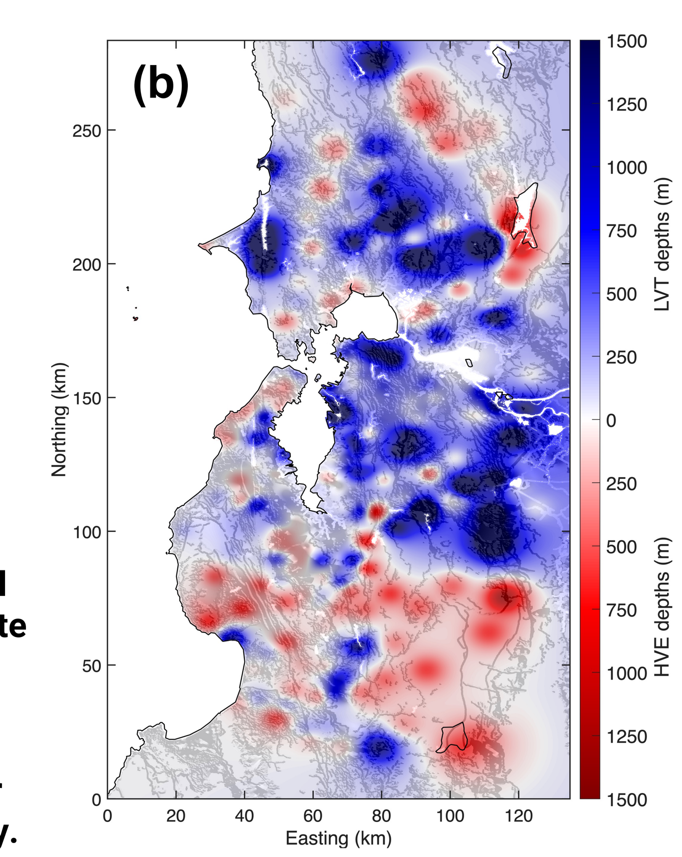

Figure 5: Site-specific optimization and spatial distribution of taper depths. (a) Mean composite error (ξ) at station J042 (see Fig. 1 for station location). (b) Spatially variable taper model, where blue and red indicate selected LVT and HVE depths, respectively. Maximum depths for LVT and HVE are 4 km and 1.5 km, respectively.

Results: Spatially Variable Taper Depths

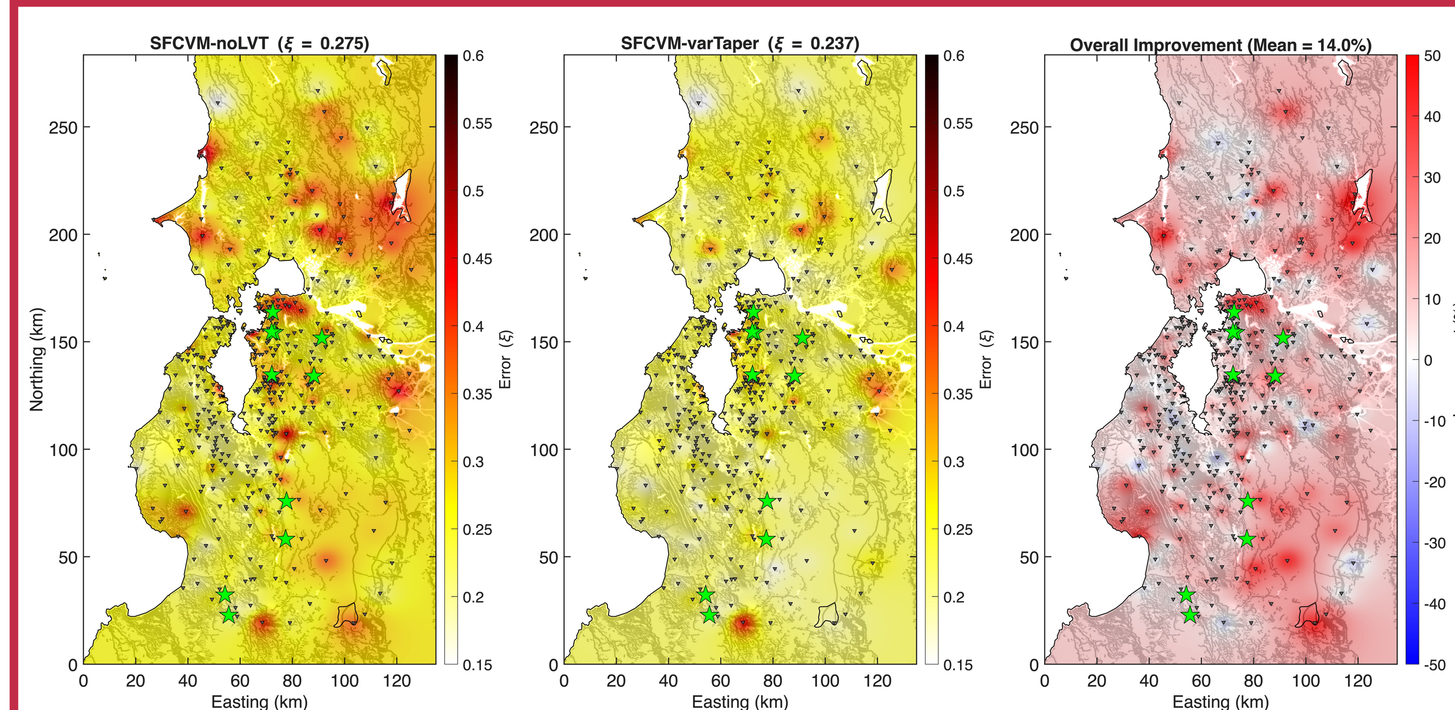

Figure 6: Ensemble error metrics for 10 events simulated using the SFCVM without LVT (left), with spatially variable taper depths (middle), and the fitness improvement from the variable taper relative to the reference model (right).

For the 10-event calibration ensemble, spatially variable taper depths reduce the composite error by an average of 14% across all sites.

The optimized model reduces mean average bias (MAB) by approximately 40% relative to the four leading NGA-W2 GMMs at periods of 2, 3, and 4 s.

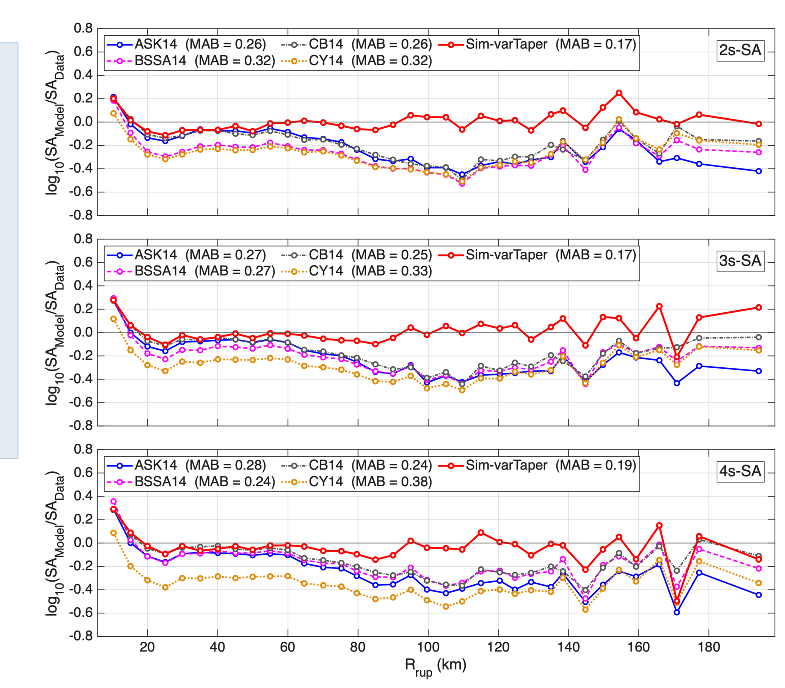

Figure 7: Ensemble-averaged SA residuals versus R_{rup} for four leading NGA-West2 GMMs and the optimized SFCVM at T = 2, 3, and 4 s.

Model Parameters

Model dimensions	Top mesh: 1800 x 3780 x 192 Bottom mesh: 600 x 1260 x 352
Grid spacings	Top mesh (dh = 75 m): Free surface - 14.25 km depth Bottom mesh (dh = 225 m): 13.725 km - 92.7 km depth
Minimum Vs	450 m/s
Maximum frequency	1 Hz
Qs/Vs	0.1
Simulated time	100 sec
Computational resources	4 SUs per hour for a run using 4 GPUs on Vista TACC

Conclusions

- The reference SFCVM (v26) requires site-specific calibration to accurately model 0–1 Hz ground motions.
- LVT depths up to 4000 m effectively mitigate underpredicted ground motions, whereas HVE depths up to 1500 m improve localized overpredictions.
- A spatially variable taper depth increases the fitness by an average of 14% across all sites, with improvements of up to 22% at sites where tapering was applied.
- The depth to the isosurface of Vs = 1.0 km/s ($Z_{1.0}$) in the SFCVM is increased by up to ~ 200 m outside the basins due to the implementation of the variable taper depth.
- The optimized model outperforms GMMs at T = 2, 3, and 4 s by ~40%.

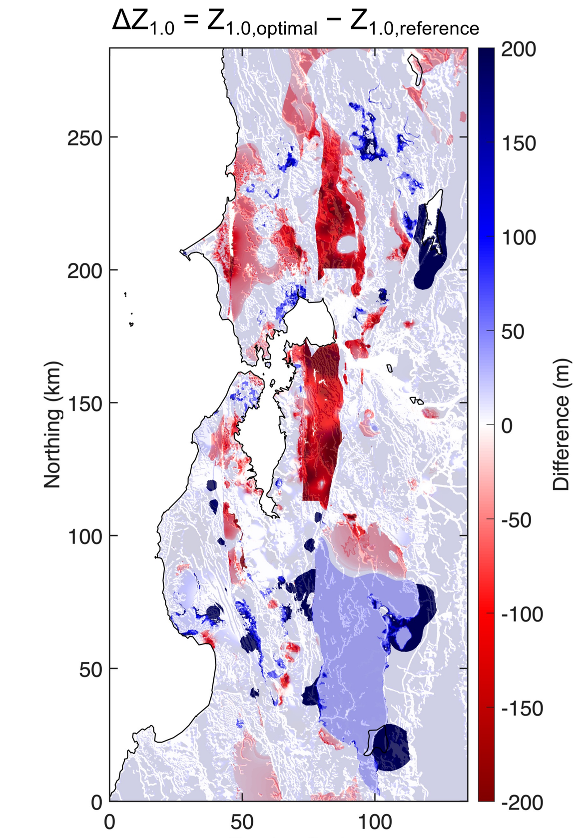

Acknowledgements

This research was supported by the Statewide California Earthquake Center (Award No. 25291). SCEC is funded by NSF Cooperative Agreement EAR-2225216 and USGS Cooperative Agreement G24AC00072. Visit www.scec.org/about/acknowledgements for more guidance

References

- Cui, Y, E. Poyraz, K.B. Olsen, J. Zhou, K. Withers, S. Callaghan, J. Larkin, C. Guest, D. Choi, A. Chourasia, Z. Shi, S. Day, P. Maechling and T.H. Jordan (2013). Physics-based seismic hazard analysis on petascale heterogeneous supercomputers. DOI: 10.1109/SC.2010.45.
- Ely, G., Small, P., Jordan, T.H., Maechling, P.J. & Wang, F. (2010). A Vs30-derived Near-surface Seismic Velocity Model, AGU Fall Meeting, S51A-1907.
- Hu, Z., K. B. Olsen, and S. M. Day (2022). Calibration of the near-surface seismic structure in the SCEC community velocity model version 4, Geophys. J. Int. 230, no. 3, 2183–2198, doi: 10.1093/gji/ggac175.
- Nie, S., Y. Wang, K.B. Olsen and S.M. Day (2017) Fourth-order staggered-grid finite-difference seismic wavefield estimation using a discontinuous mesh interface (WEDMI) fourth order staggered-grid finite-difference seismic WEDMI. Bull. Seis. Soc. Am. 107, 2183–2193.
- O'Reilly, O., T.-Y. Yeh, K.B. Olsen, Z. Hu, A. Breuer, D. Roten, and C. Goulet (2022). A high-order finite difference method on staggered curvilinear grids for seismic wave propagation applications with topography. Bull. Seis. Soc. Am. 112 (1), 3-22. doi.org/10.1785/0120210096
- Thompson, E.M., (2018). An Updated Vs30 Map for California with Geologic and Topographic Constraints (ver. 2.0, July 2022): U.S. Geological Survey data release, https://doi.org/10.5066/F7JQ108S.